Magnetic Gold Nanoshells: Step-wise Changing of Magnetism through Step-wise Biofunctionalization

Challa S.S.R.Kumar[1,*] and **Faruq Mohammad**[1,2]

[1]Center for Advanced Microstructures & Devices, Louisiana State University, 6980 Jefferson Highway, Baton Rouge, LA 70806. USA

[2]Environmental Toxicology, Southern University and A&M College, Baton Rouge, LA 70813, USA

Abstract

We report step-wise changing of magnetic behavior of iron oxide core gold shell nanoparticles from super paramagnetic to permanent magnetism at room temperature, on step-wise bio-functionalization with leutenizing hormone and releasing hormone (LHRH) through cysteamine linker. The observed permanent magnetism at room temperature in LHRH-capped gold nanoshells provides opportunities to extend fundamental investigations of permanent magnetism to other novel nanostructures and biofunctionalized nano gold architectures, simultaneously opening the way to newer applications, especially to those in biomedicine.

Keywords

Iron oxide nanoparticles; SPION; Gold nanoshell; SPION@Au; Thiol capping; leutenizing hormone and releasing hormone (LHRH); Biofunctionalization

It is well known that bulk gold is diamagnetic due to counteraction of paramagnetic behavior of conduction electrons by orbital and ionic core diamagnetism. On the other hand, single gold atoms are paramagnetic because of the unpaired 6s electron.[1] There is a distinct change in the magnetism as one goes from gold atoms to nano gold and further to bulk gold and these fundamental changes in the magnetism are interesting from basic research as well as practical applications. Adding to this is recently reported chemically induced ferromagnetism in thiol-capped gold nanoparticles.[2] The chemically induced permanent magnetism was also extended to Ag and Cu nano clusters.[3] The surprising induction of permanent magnetism, under some conditions of chemisorptions, in small nanoparticles of a bulk-diamagnetic metal is likely through an interaction of s and p orbitals of adsorbates such as thiolates with 5d-orbitals of metal atoms. This interaction is anticipated to lead to emergence of 5d-localized holes as a result of significant charge transfer occurring from the metal atoms to sulfur atoms in the adsorbate molecule. The Au L3-edge extended X-ray absorption near-edge structure (EXAFS) measurements confirm the existence of these holes in Au nanoparticles capped with thiolates.[4, 5] This interaction between the orbitals of S and Au is ultimately responsible for the onset of magnetism in thiol-capped gold nanoclusters. Recent literature reports indicate that different types of thiol-capped Au nanoparticles showed a great variety of effects going from giant paramagnetism,[6] superparamagnetism,[7] and even to permanent magnetism.[2, 8]

While majority of the investigations on magnetism of thiol-capped Au clusters involve thiols, potential magnetism associated with S-Au bonding through amino acid capping of Au clusters has not been examined.[9] Surprisingly, magnetism in thiol-capped gold nanoshells especially those with the core-shell architecture has not been demonstrated. Magnetic investigation of gold nanoshells is very interesting as it will address a number of questions: if the magnetic behavior of gold atoms is influenced by a core and a shell. Yet another important question that arises from the view point of biomedical applications is whether gold nanoshells chemisorbed with biologically significant thiolated amino acids, peptides and nucleic acids will show permanent magnetism or not. In order to tackle these questions, we have synthesized in three steps luteinizing hormone releasing hormone (LHRH)-capped gold coated super paramagnetic iron oxide nanoparticles (SPIONs) providing us with a structure that has Au atoms between the super paramagnetic iron oxide core and diamagnetic cysteamine and LHRH ligand. The reason for choosing LHRH is that majority types of human cancers express receptors for LHRH [10]-[13] and we have recently demonstrated that LHRH bound to iron oxide nanoparticles are extremely sensitive magnetic resonance imaging (MRI) contrast agent for the detection of primary as well as metastatic breast cancer cells.[14]-[15]

We synthesized SPIONs (Fe_3O_4) and gold coated SPIONs ($Fe_3O_4@Au$) modifying the procedure described previously.[16] The SPIONs@Au nanoparticles were purified magnetically making them free of unwanted residual amount of pure Au nanoparticles. The HRTEM measurements show their spherical nature and the mean size of SPIONs@Au is 6.3 ± 0.7 nm compared to 5.4 ± 0.4 nm for SPIONs (Figure 1 and S1). The particles are well dispersible in toluene and their UV-Visible absorption spectra showed a clear surface plasmon resonance (SPR) band at 558 nm (Figure S3) which is the characteristic optical property of gold nanostructures confirming that the core Fe_3O_4 is coated with Au shell. Small angle-X-ray scattering analysis (SAXS) was carried out using CAMD's synchrotron beam line (www.camd.lsu.edu). Figure-S2 shows the SAXS data for both coated and uncoated SPIONs. The mean particle diameters determined from the SAXS data were 4.6 ± 0.4 and 5.3 ± 0.4 nm for SPIONs and SPIONs@Au respectively (Figure S2).[17] From both HRTEM and SAXS data, the observed difference in diameter between coated and uncoated samples suggests formation of a gold shell of approximately 0.4 to 0.5 nm thickness. It is to be noted that the atomic diameter of gold is 0.288 nm and the observed difference in the size of SPIONs and SPIONs@Au corresponds to approximately twice this value as expected. More detailed characterization on SPION@Au nanoparticles and their ability to enhance hyperthermia by four- to five-fold in comparison with SPIONs was recently reported.[18]

The SPIONs@Au nanoparticles were first functionalized with cysteamine taking advantage of formation of a strong S-Au bond. This was followed by functionalization with LHRH peptide using carbodiimide activation. The SPIONs@Au-Cysteamine-LHRH particles were found to be magnetic and also show SPR band confirming the presence of SPION core and Au shell. A schematic representation of step-wise bio-functionalization process is depicted in Figure 2 and the synthetic procedure is provided in the experimental section. As seen from Figure 1, the core-shell particles remain well separated without any agglomeration after each stage of step-wise bio-functionalization.

SPR is a powerful tool for analysis of changes occurring in the electronic configuration of nanoparticles due to surface effects. Especially in the case gold nanoshells with a silica core have attracted a lot of attention because their surface plasmon resonance (SPR) peaks can be widely tuned from the visible to the infrared region by engineering the shell structure.[19] Based on a number of theoretical and experimental studies that such shifts in plasmon resonance of the gold nanoparticles takes place as the particles come together.[20] In our case, we observe a bathochromic shift (558 to 567 nm) on exchanging oleic acid/oleyl amine with

cysteamine onto gold nano shell. The SPR band remains same on binding LHRH to cysteamine (566 nm) (Figure S3). Figure S4 shows the FT-IR comparison of surface functional groups in samples (a), (b), (c), and (d). The SPR studies also supports that the particles remain isolated with no aggregation or agglomeration at each step of the bio-functionalization process. A detailed infra red spectroscopy analysis was carried to confirms step-wise biofunctionalization process on the gold nanoshell (Figure S4). The absence of the –SH stretching vibration at 2550 cm^{-1} and bending vibration at 764 cm^{-1} in SPIONs@Au-Cysteamine when compared with pure cysteamine confirms formation of S-Au bond on gold surface. The presence of a sharp peak in cysteamine bound SPIONs@Au at 1624 cm^{-1} due to strong in plane –NH_2 scissoring absorptions which changed to a broad peak at 1647 cm^{-1} in SPIONs@Au-Cysteamine-LHRH confirms binding of LHRH to SPIONs@Au-Cysteamine. This is supported by the peak due to C-N stretching vibration changing from 1251 to 1261 cm^{-1} and the N-H bending vibration peak in SPIONs@Au-Cysteamine at 806 cm^{-1} changing to a weak broad peak at 804 cm^{-1} after binding to LHRH.[21]-[22] The binding of cysteamine to Au shells and LHRH to cysteamine is also confirmed by XPS studies (Figure S5).

Magnetic characterization of the samples was carried out using a superconducting quantum interference device (SQUID) magnetometer. Figure 3(a) shows both zero field cooled (ZFC) and field cooled (FC) temperature dependent magnetization curves for SPIONs@Au-Cysteamine and SPIONs@Au-Cysteamine-LHRH. The blocking temperature changes from 201.5 K to >300 K on binding SPIONs@Au-Cysteamine with LHRH. These changes are dramatic when compared with that of SPIONs and gold coated SPIONs (19.1 K and 44.3 K respectively). A step-wise increase in Tb is seen from SPIONs > SPIONs@Au > SPIONs@Au-Cysteamine >SPIONs@Au-Cysteamine-LHRH finally leading to permanent magnetism in SPIONs@Au-Cysteamine-LHRH. This is also supported by the room temperature hysteresis data. Figure 3(b) shows the hysteresis loops for SPIONs@Au-Cysteamine and SPIONs@Au-Cysteamine-LHRH at 5 K and 300 K. An expanded plot is shown in the inset. While SPIONs, SPIONs@Au and SPIONs@Au-Cysteamine exhibit superparamagnetism, the SPIONs@Au-Cysteamine-LHRH shows hysteresis at room temperature. The presence of non zero coercivity and a non zero remanance ratio (Mr/Ms=0.012) at room temperature indicates existence of residual magnetic moment in SPIONs@Au-Cysteamine-LHRH conforming its ferromagnetic behavior (Table S1). It is also interesting to note that on binding of cystemaine to the Au surface there is a dramatic increase in magnetic moment of core-shell particles. The value of magnetic moment per Au atom bound to sulfur (practically all the gold atoms in the shell) can be estimated to be ~180 μ_B, B being the Bohr magneton. This is extremely high in comparison with magnetic moment per Au atom recently reported in the case of dodecane thiol stabilized gold clusters < 2nm.[3] On the other hand, on further functionalization with LHRH, the magnetic moment per Au atom decreases and is on par with that of gold coated SPIONs. The decrease in the magnetic moment could be due to contribution of overall mass from the nonmagnetic LHRH peptide, whose molecular weight is 1182.29. Yet another explanation for this reduction in magnetic moment is due to the fact that the surface magnetic order can be affected by structural distortions that cause spin canting.[23] Also, a careful review of literature shows variations in magnetism in organically capped Au and other metal nanoclusters and there are no identical publications reporting the same magnetic behavior. A broad range in the calculated values of magnetic moments for magnetic Au reported to date ranges from is 0.002 to 0.036 μ_B. One possible explanation for these differences could be that variation in nature of thiol bonding on the surface Au atoms due to different thiol functional groups leads to changes in the generation of holes in the 5d energy level. However, it is obvious that further work is necessary to understand the chemical and physical mechanisms behind different types of Au-thiol bonds in order to arrive at correct explanation for their magnetic behavior.

The magnetic data thus demonstrate that there is a step-wise change in magnetic properties of Au nanoshells on step-step-wise biofunctionalization. The significant change in the magnetic properties of cysteamine bound Au nanoshells compared to gold nanoshells can be due to modification of Au electronic structure on introduction Au-S bond. Such a change in magnetism is well documented and is explained based on induction of 5d band holes localized in the vicinity of thiol bond and subsequent lattice expansion with respect to bulk Au.[3],[4],[5] However, a further shift in magnetism to ferromagnetism at room temperature on binding with LHRH is at first intriguing. It has been recently reported that electron/hole density at d band of Au clusters is influenced by the nature of capping system.[24] It is, therefore, possible that modifying the capping agent from cysteamine to cystemaine-LHRH is influencing the S-Au bond through electron/hole density at d band of Au clusters; which in turn has influence on magnetic properties. Further work is in progress to quantitatively understand the influence of bio-functionalization on magnetism of gold nanoshells for potential application in biosensing.

In conclusion, while a large number of recent publications have been reporting magnetism of thiol capped small Au clusters, we report a step-wise change in magnetism of gold nanoshells with stepwise changes in thiol functionalization. The work reported here also demonstrates that, similar to small Au clusters, chemically induced permanent magnetism is possible in gold nanoshells. It is anticipated that the physical mechanism associated with magnetism in thiol-capped Au nanoshells can be extended to other types of gold structures, [25] opening the door for newer possibilities of understanding the fundamental questions in magnetism in addition to yet to discover applications.

EXPERIMENTAL METHODS

SPIONs

Briefly, 0.71 grams of iron acetylacetonate was mixed with 20 ml of phenyl ether, 2 ml of oleic acid and 2ml of oleylamine under inert atmosphere with vigorous stirring. 2.58 g of 1,2 hexadecanediol was added to the solution. The solution was heated to around 210 °C with reflux for 2 h maintaining oxygen free conditions. The reaction mixture was cooled to room temperature and then ethanol (degassed) was added to precipitate the black colored product. The precipitate was separated out by centrifugation. The precipitated product was then washed with a series of solvents starting with hexane, followed by a mixture of hexane & ethanol and then finally with ethanol. The product was dispersed in ethanol and separated magnetically and dried to obtain a black powder which could be well dispersed in tolune.

SPIONs@Au

To 10 ml of phenyl ether, approximately 0.5 g of SPIONs was added. To this mixture a solution containing 30 ml of phenyl ether, 3.1 g of 1,2 hexadecanediol, 0.5 ml of oleic acid, 3 ml of oleylamine and 0.83 g of gold acetate was added under inert atmosphere. The reaction mixture was heated to around 190 °C with reflux for about 1.5 h. After cooling to room temperature, ethanol was added and the dark purple material was separated out by centrifugation. The material was resuspended in hexane, washed with ethanol 2-3 times and dried. With the help of magnetic separation technique, by suspending the particles in ethanol, the magnetic gold coated iron oxide nanoparticles were separated from the non magnetic gold NPs and any unwanted carbon mass produced from oleic acid/oleylamine used during the course of the reaction.

Characterization SPIONs@Au nanoparticles

High resolution transmission electron microscopy (HRTEM) analyses were carried out by using JEOL-2010 HRTEM instrument with a point to point resolution of 1.94 Å, operated at

200 kV accelerating voltage. The magnetic measurements were conducted using a Quantum Design MPMS-5S superconducting quantum interference device (SQUID) magnetometer. Small angle X-ray scattering (SAXS) measurements were carried out at the Center for Advanced Microstructures and Devices (CAMD) with synchrotron radiation of wavelength, $\lambda = 1.55$ Å. The SPIONs were dispersed in toluene and sealed in glass capillaries. The scattering pattern was imaged with a two dimensional Gabriel style multi-wire gas detector with a 200 mm active diameter and a resolution of 200-250 μm FWHM in a 1024×1024 array. The sample and the detector chamber were kept under vacuum during the measurements to maximize the intensity and to minimize the scattering from air. Scattering curves were monitored in a Q-range from 0.0066 to 0.164 Å^{-1}. Azimuthally averaged data from the detector were normalized for average transmitted intensity and corrected for background. X-ray photoelectron spectroscopy (XPS) analyses were done on AXIS 165 High Performance multi-technique surface analyzer which is based on a 165mm mean radius hemispherical analyzer, with an eight channeltron detection system. For UV-Visible spectroscopy, QE65000 spectrometer supplied by Ocean Optics limited was used and the samples were dispersed in toluene for SPIONs, SPIONs@Au and in water for SPIONs@Au-Cysteamine, SPIONs@Au-Cysteamine-LHRH. The thermal stability of the samples was analyzed by using thermogravimetric analysis (TGA). Starting from room temperature, the samples were heated upto 600 °C at a rate of 10 °C per min on a TA 600 instrument.

Binding of SPIONs@Au with LHRH

For the synthesis of LHRH bound SPIONs@Au, we prepared first the cysteamine bound SPIONs@Au followed by the binding reaction with LHRH. First, to 30 mg of SPIONs@Au, 10 ml of toluene was added and shaken thoroughly. In another flask, 10 mg of cysteamine hydrochloride solution in 10 ml of distilled water was prepared. Both the solutions were added together and stirred for about 10 minutes. At first we see clearly two phases with the bottom colorless due to water and the top purple colored toluene containing the nanoparticles; after 2-4 hours of time, we see the migration of nanoparticles into the cysteamine water phase. The cysteamine bound SPIONs@Au were separated using a magnetic separator, washed 2-3 times with distilled water and dried under inert atmosphere.

60 mg of SPIONs@Au-Cysteamine in 16 ml of distilled water was added to 42 mg of EDC (1-ethyl-3-(3-dimethylaminopropyl) carbodiimide) in 1.5 ml of distilled water, and sonicated for 3 minutes. To this reaction mixture, 3.7 mg of LHRH (with free carboxylic group) dissolved in 1.5 ml of distilled water was added and stirred in chiller for about 2 hours to maintain a constant temperature of 4 °C. After that the LHRH bound SPIONs@Au-Cysteamine were separated by centrifugation, washed with distilled water for several times to separate the unbound LHRH and any other unreacted EDC.

Supplementary Material

Refer to Web version on PubMed Central for supplementary material.

Acknowledgments

References

1. White, RM. Quantum Theory of Magnetism. 3. New York: Springer. 2007

2. Crespo P, Litrán R, Rojas TC, Multigner M, de la Fuente JM, Sánchez-López JC, García MA, Hernando A, Penadés S, Fernández A. Permanent Magnetism, Magnetic Anisotropy, and Hysteresis of Thiol-Capped Gold Nanoparticles. Phys Rev Lett. 2004; 93:087204–087207. [PubMed: 15447222]

3. Garitaonandia JS, Insausti M, Goikolea E, Suzuki M, Cashion JD, Kawamura N, Ohsawa H, Gil de Muro I, Suzuki K, Plazaola F, Rojo T. Chemically induced permanent magnetism in Au, Ag and Cu nanoparticles: localization of the magnetism by element selective techniques. Nano Lett. 2008; 8:661–667. [PubMed: 18215085]

4. Zhang P, Sham TK. X-Ray Studies of the Structure and Electronic Behavior of Alkanethiolate-Capped Gold Nanoparticles: The Interplay of Size and Surface Effects. Phys Rev Lett. 2003; 90:245501 (4pp). [PubMed: 12857199]

5. Gonzalez C, Simón-Manso Y, Marquez M, Mujica V. Chemisorption-induced spin symmetry breaking in gold clusters and the onset of paramagnetism in capped gold nanoparticles. J Phys Chem B. 2006; 110:687–691. [PubMed: 16471589]

6. Carmeli I, Leitus G, Naaman R, Reich S, Vager Z. Magnetism induced by the organization of self-assembled monolayers. J Chem Phys. 2003; 118:10372–10375.

7. Dutta P, Pal S, Seehra MS, Anand A, Roberts CB. Magnetism in dodecanethiol-capped gold nanoparticles: Role of size and capping agent. Appl Phys Lett. 2007; 90:213102.

8. De la Venta J, Pucci A, Fernández Pinel E, García MA, de Julián Fernández C, Crespo P, Mazzoldi P, Ruggeri G, Hernando A. Magnetism in Polymers with Embedded Gold Nanoparticles. Adv Mater. 2007; 19:875–877.

9. Sun Q, Reddy BV, Marquez M, Jena P, Gonzalez C, Wang Q. Theoretical study on gold coated iron oxide nanostructure: Magnetism and bioselectivity for amino acids. J Phys Chem C. 2007; 111:4159–4163.

10. Lojun S, Bao S, Lei ZM, Rao CV. Presence of functional luteinizing hormone/chorionic gonadotropin (hCG) receptors in human breast cell lines: implications supporting the premise that hCG protects women against breast cancer. Biol Reprod. 1997; 57:1202–1210. [PubMed: 9369188]

11. Chatzistamou L, Schally AV, Nagi A, Szepeshazi K, Halmos G. Effective treatment of metastatic MDA-MB-435 human estrogen-independent breast carcinomas with a targeted cytotoxic analogue of luteinizing hormone-releasing hormone AN-207. Clin Cancer Res. 2000; 6:4158–4168. [PubMed: 11051271]

12. Leuschner C, Enright F, Gawronska B, Hansel W. Membrane disrupting lytic peptide conjugates destroy hormone dependent and independent breast cancer cells in vitro and in vivo. Breast Cancer Res Treat. 2003; 78:17–27. [PubMed: 12611453]

13. Leuschner C, Hansel W. Targeting breast and prostate cancers through their hormone receptors. Biol Reprod. 2005; 73:255–260.

14. Branca T, Cleveland ZI, Leuschner C, Kumar C, Fubara B, Maronpot RR, Warren W, Driehuys B. Molecular MRI for sensitive and specific detection of lung metastases. Proc Natl Acad Sci. 2010; 107:3693–3697. [PubMed: 20142483]

15. Leuschner C, Kumar CSSR, Jikou Z, Soboyejo WO, Hansel W, Hormes J. LHRH-conjugated magnetic iron oxide nanoparticles for detection of breast cancer metastases. Breast Cancer Res Treat. 2006; 99:163–176. [PubMed: 16752077]

16. Wang L, Luo J, Fan Q, Suzuki M, Itsuko S, Suzuki M, Engelhard H, Yuehe L, Nam K, Wang JQ, Zhong CJ. Monodispersed Core-Shell Fe_3O_4@Au Nanoparticles. J Phys Chem B. 2005; 109:21593–21601. [PubMed: 16853803]

17. Bonini M, Fratini E, Baglioni P. SAXS study of chain-like structures formed by magnetic nanoparticles. Mater Sci Eng C. 2007; 27:1377–1381.

18. Mohammad F, Balaji G, Weber A, Uppu RM, Kumar CSSR. Influence of Gold Nanoshell on Hyperthermia of Super Paramagnetic Iron Oxide Nanoparticles (SPIONs). J Phys Chem C. in press.

19. Zhang Q, Ge J, Goebl J, Hu Y, Sun Y, Yin Y. Tailored Synthesis of Superparamagnetic Gold Nanoshells with Tunable Optical Properties. Adv Mater. 2010; 22:1905–1909. [PubMed: 20526992]

20. Jain PK, El-Sayed MA. Universal Scaling of Plasmon Coupling in Metal Nanostructures: Extension from Particle Pairs to Nanoshells. Nano Lett. 2007; 7(9):2854–2858. [PubMed: 17676810]

21. Shukla N, Chao L, Jones PM, Weller D. FTIR study of surfactant bonding to FePt nanoparticles. J Magn Magn Mater. 2003; 266:178–184.

22. Nandy SK, Mukherjee DK, Roy SB, Kastha GS. Vibrational Spectra and Rotational Isomerism in 2-Mercaptoethanol. Can J Chem. 1973; 51:1139–1141.

23. Morales MP, Veintemillas-Verdaguer S, Montero MI, Serna CJ, Roig A, Casas L, Martinez B, Sandiumenge F. Surface and Internal Spin Canting in γ-Fe_2O_3 Nanoparticles. Chem Mater. 1999; 11:3058–3064.

24. López-Cartes C, Rojas TC, Litrán R, Martínez-Martínez D, de la Fuente GM, Penadés S, Fernández A. Gold nanoparticles with different capping systems: An electronic and structural XAS analysis. J Phys Chem B. 2005; 109:8761–8766. [PubMed: 16852039]

25. Shultz MD, Calvin S, Gonzalez-Jimenez F, Mujica V, Alleluia BC, Carpenter EE. Gold-Coated Cementite Nanoparticles: An Oxidation-Resistant Alternative to r-Iron. Chem Mater. 2009; 21:5594–5600.
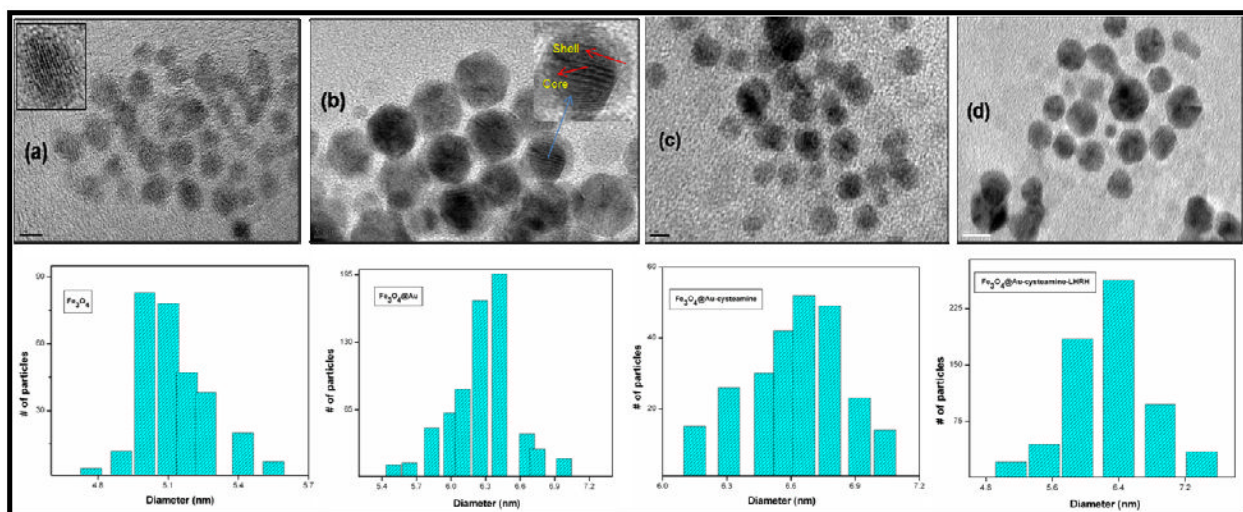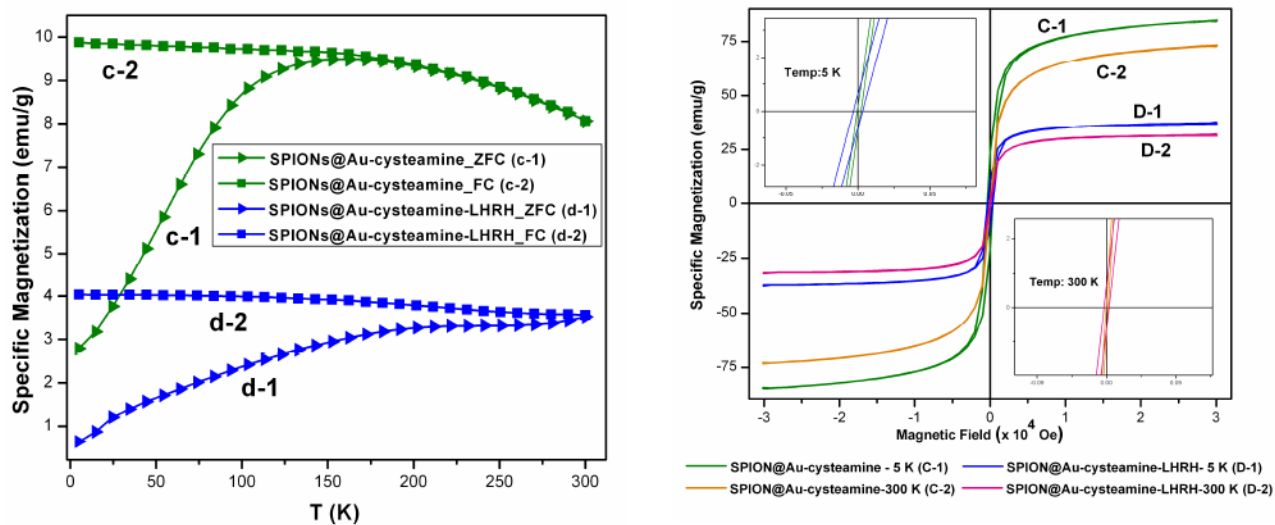
Figure 1.
HRTEM images and size distribution for SPIONs (a), SPIONs@Au (b), SPIONs@Au-Cysteamine (c) and SPIONs@Au-Cysteamine-LHRH (d). From the HRTEM data, the mean size distributions of these particles were found to be in the order of 5.4 ± 0.4, 6.3 ± 0.7, 6.6 ± 0.7, and 6.7 ± 0.8 respectively. (HRTEM bar scale: (a) 5 nm, (b) 2 nm, (c) 5 nm, and (d) 10 nm)
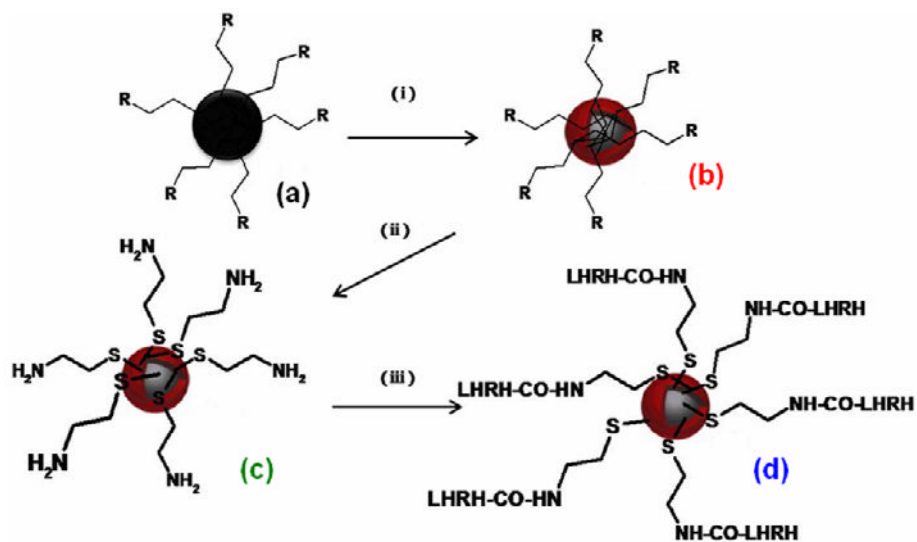
Figure 2.
A schematic of step-wise gold nanoshell formation followed by biofunctionalization. (i)
Gold acetate/oleic acid/oleylamine (R=oleic acid/oleylamine) (ii) Cysteamine hydrochloride
(iii) LHRH/EDC at 4 °C. (a) SPIONs (b) SPIONs@Au (c) SPIONs@Au-Cysteamine and
(d) SPIONs@Au-Cysteamine-LHRH.

Figure 3.
(a:left) ZFC/FC curves for SPIONs@Au-Cysteamine (c) and SPIONs@Au-Cysteamine-LHRH (d) respectively. (b: right) Hysteresis curves at 5K and 300K (top left inset at 5K and bottom right inset at 300K) for SPIONs@Au-Cysteamine (C) and SPIONs@Au-Cysteamine-LHRH (D) respectively.